

pubs.acs.org/JACS Article

# Derivatized Benzothiazoles as Two-Photon-Absorbing Organic Photosensitizers Active under Near Infrared Light Irradiation

Bidyut Kumar Kundu, Guanqun Han, and Yujie Sun\*



Cite This: J. Am. Chem. Soc. 2023, 145, 3535-3542



**Read Online** 

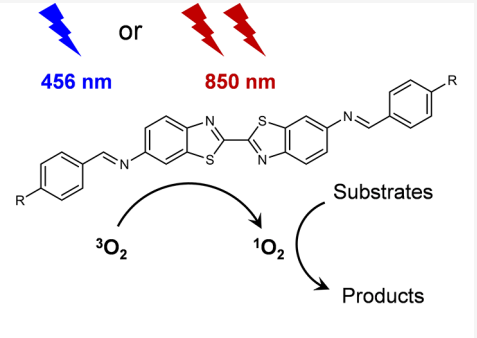
**ACCESS** 

III Metrics & More

Article Recommendations

s Supporting Information

**ABSTRACT:** Homogeneous organic photocatalysis typically requires molecular photosensitizers absorbing in the ultraviolet—visible (UV/vis) region, because UV/vis photons possess the sufficient energy to excite those one-photon-absorbing photosensitizers to the desired excited states. However, UV/vis light irradiation has many potential limitations, especially for large-scale applications, such as low penetration through reaction media, competing absorption by substrates and cocatalysts, and incompatibility with substrates bearing light-sensitive functionalities. In fact, these drawbacks can be effectively avoided if near infrared (NIR) photons can be utilized to drive the target reactions. Herein, we report two benzothiazole-derived compounds as novel two-photon-absorbing (TPA) organic photosensitizers, which can function under NIR light irradiation using inexpensive LED as the light source. We demonstrate that by judicially modulating the donor- $\pi$ -acceptor- $\pi$ -donor-conjugated structure containing a bibenzothiazole



Organic two-photon-absorbing photosensitizers

core and imine bridges, excellent two-photon absorption capability in the NIR region can be achieved, approaching 2000 GM at 850 nm. Together with large quantum yields ( $\sim$ 0.5), these benzothiazole-derived TPA organic photosensitizers exhibit excellent performance in driving various  $O_2$ -involved organic reactions upon irradiation at 850 nm, showing great penetration depth, superior to that upon blue light irradiation. A suite of photophysical and computational studies were performed to shed light on the underlying electronic states responsible for the observed TPA capability. Overall, this work highlights the promise of developing Ru/Ir-free organic photosensitizers operative in the NIR region by taking advantage of the two-photon absorption mechanism.

#### INTRODUCTION

Organic photocatalysis merges organic synthesis with photochemistry and enables many challenging organic transformations to take place under ambient conditions while using photon as the sole energy source. 1-4 The last two decades have witnessed an exponential growth in this field, and it has been widely recognized that there is a great potential for the utilization of organic photocatalysis in large-scale industrial processes.<sup>5,6</sup> Due to their rich photophysical and photochemical properties, expensive ruthenium and iridium complexes have been the dominant photosensitizers in reported organic photocatalysis.<sup>7-9</sup> However, if organic photocatalysis is to be adopted for large-scale applications, it is more desirable to replace those noble metal chromophores with more earth-abundant, less expensive, and non-toxic photocatalysts. In this regard, homogeneous organic photosensitizers have attracted increasing attention as promising alternatives, because they display tunable photophysical and photochemical properties via nearly endless structural modification strategies.

In conventional organic photocatalysis, ultraviolet and/or visible (UV/vis) light irradiation is nearly mandatory for all the molecular photosensitizers, because high-energy photons are required to excite those one-photon-absorbing chromophores to the desired excited states.  $^{10-12}$  However, UV/vis light only

covers a limited portion of the solar spectrum and also has many intrinsic limitations such as low penetration through reaction media, 13-15 potential competing absorption by substrates and co-catalysts, 16-18 and incompatibility with substrates bearing light-sensitive functionalities. 19 Even though these challenges can be overcome by the use of near infrared (NIR) photons, NIR light-absorbing photosensitizers have been rarely utilized. A survey of over 60 reported organic photosensitizers indicates that most of those chromophores only absorb in the UV and short visible region with the lowest energy absorption maximum falling between 300 and 500 nm. 20-22 Even though a few red and NIR light-absorbing organic photosensitizers have been reported, 23,24 because of the energy gap law, their quantum yields and excited-state lifetimes are usually small, potentially limiting their practical applications.

Received: November 17, 2022 Published: February 2, 2023





As shown in Figure 1, there are two possible strategies to produce a high-energy excited state while still absorbing in the

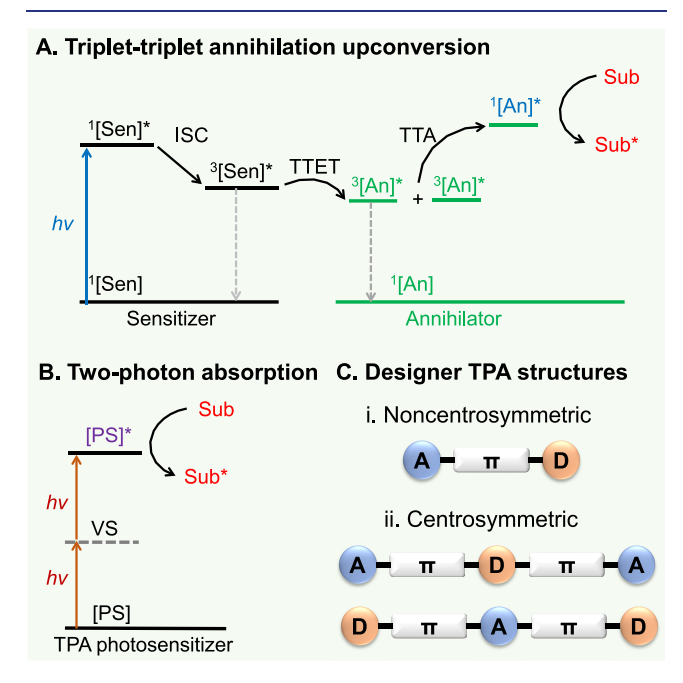


**Figure 1.** (A) Schematic illustration of triplet—triplet annihilation upconversion. (B) Two-photon absorption. [Sen]: sensitizer; [An]: annihilator; ISC: intersystem crossing; TTET: triplet—triplet energy transfer; TTA: triplet—triplet annihilation; [PS]: photosensitizer; [Sub]: substrate. (C) Designer structures of TPA complexes. D: electron-donating moiety; A: electron-accepting moiety;  $\pi$ :  $\pi$ -conjugated linker.

NIR region: (i) triplet-triplet annihilation upconversion (TTA-UC) and (ii) direct two-photon absorption (TPA). Figure 1A depicts the process of TTA-UC, which involves two species: sensitizer ([Sen]) and annihilator ([An]).<sup>25-28</sup> The sensitizer is preferred to have intense absorption in the NIR region accompanied by long lifetime of its triplet excited state, whose energy is transferred to the annihilator, forming  ${}^{3}[An]^{*}$ . Next, two <sup>3</sup>[An]\* species undergo triplet fusion resulting in the generation of one higher-energy singlet annihilator, <sup>1</sup>[An]\*, that is able to perform the desirable function, while the other <sup>3</sup>[An]\* decays to its ground state. Overall, the success of TTA-UC relies on the fine energy matching and intimate interaction of the sensitizer and annihilator. Even though this strategy has been recently employed in organic photocatalysis, 26,27 its wide application may be restricted by its complex nature and the availability of suitable pairs of sensitizers and annihilators. In contrast, the TPA strategy requires only one molecule capable of absorbing two low-energy photons to populate its desired excited state (Figure 1B).<sup>29,30</sup> In fact, the power of TPA complexes has been manifested in a wide range of fields, including imaging, 31,32 sensing, 33 and information storage. 34,35 However, organic TPA photosensitizers have received scarce attention for photocatalysis, probably because most reported organic photosensitizes only exhibit limited TPA capability.

Built upon the seminal works of Webb et al. in designing and investigating organic TPA molecules<sup>36</sup> and the recent development in this field,<sup>34,37</sup> we reasoned that organic molecules with prominent intra-molecular charge transfer are likely to exhibit appreciable two-photon absorption in the NIR region. Figure 1C presents the designer models of potential TPA molecules

with non-centrosymmetric dipolar structures and centrosymmetric quadrupolar structures. 38-40 Encouraged by the recently reported results on benzothiazole-derived organic chromophores, which possess an excellent TPA cross section  $(\sigma_2)$  in the NIR region,  $^{41-43}$  we were particularly interested in developing organic TPA photosensitizers consisting of a bibenzothiazole core as the electron acceptor, which is also conjugated with two terminal electron donors. Herein, we report the synthesis, characterization, and photophysical studies of two new benzothiazole-derived TPA photosensitizers, which can be successfully employed as photocatalysts in various organic reactions under NIR light (850 nm) irradiation. Because of the deeper penetration of NIR light versus visible light in reaction media, these organic TPA photosensitizers exhibit even better performance under NIR light irradiation than under blue-light irradiation in some cases. To the best of our knowledge, this is the first time that organic two-photon-absorbing compounds have been utilized as photocatalysts in driving organic transformations using inexpensive NIR LED ( $\lambda_{ex}$  = 850 nm), instead of laser, as the light source.

#### RESULTS AND DISCUSSION

The synthesis of our designed TPA photosensitizers started from a nitration step at the C-6 position of commercially purchased benzothiazole (Scheme 1), followed by reduction to

## Scheme 1. Synthetic Route of dBIP and dBIP-NMe<sub>2</sub> Starting from Benzothiazole

give 6-aminobenzothiazole. Subsequent condensation with benzaldehyde resulted in an intermediate containing an imine linker. Finally, an oxidative Sonogashira homocoupling of the imine intermediate at the C-2 position produced the target molecule dBIP. Such a synthetic route allows the facile incorporation of electron-donating substituents at the *para* position of both terminal phenyl rings in dBIP. For instance, once 4-(dimethylamino)benzaldehyde was employed to replace benzaldehyde in the above condensation step, a new product dBIP-NMe<sub>2</sub> can be readily obtained following the same synthetic strategy. The synthetic details and spectroscopic characterization (Figures S1–S11) of dBIP, dBIP-NMe<sub>2</sub>, and all the intermediates are found in the Supporting Information.

As depicted in Figure 2A, dBIP exhibits an absorption feature with a maximum at 409 nm ( $\varepsilon = 11,436 \text{ M}^{-1} \text{ cm}^{-1}$ )

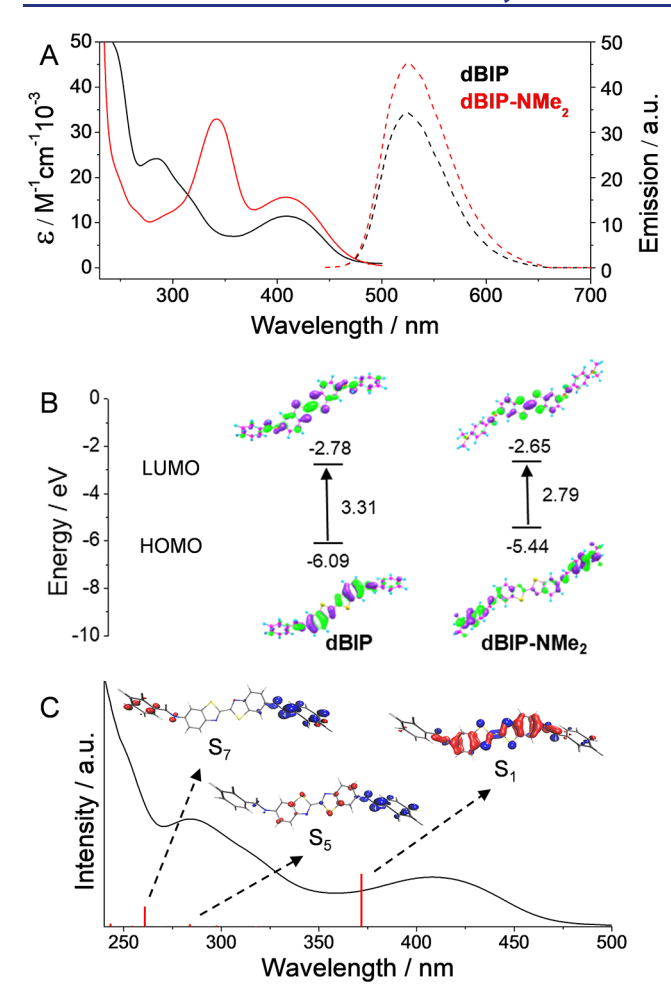


**Figure 2.** (A) UV/vis absorption and emission in CH<sub>3</sub>CN and (B) calculated frontier orbitals of **dBIP** and **dBIP-NMe**<sub>2</sub>. DFT calculations used B3LYP as a functional and 6-311+G(d,p) as a basis function. (C) Comparison between the TD-DFT calculated singlet excited states ( $S_1$ ,  $S_5$ , and  $S_7$ ) and experimental absorption spectrum of **dBIP** with selected EDDMs (isovalue = 0.04; red and blue indicate electron density decrease and increase, respectively).

and strong emission in the green region with  $\lambda_{\rm em}=513$  nm in CH<sub>3</sub>CN. The fluorescence quantum yield of **dBIP** was measured as 0.48, and its lifetime was 2.87 ns (Figure S12).<sup>45</sup> With the electron-donating dimethylamino substituents, **dBIP-NMe**<sub>2</sub> shows enhanced absorption in the blue region ( $\lambda_{\rm abs}=408$  nm,  $\varepsilon=15,626$  M<sup>-1</sup> cm<sup>-1</sup>) and a new absorption peak at 342 nm ( $\varepsilon=32,944$  M<sup>-1</sup> cm<sup>-1</sup>) in CH<sub>3</sub>CN. A slightly red-shifted emission was also observed for **dBIP-NMe**<sub>2</sub>, together with an increased quantum yield of 0.51 and a lifetime of 2.89 ns (Figure S12).

Density functional theory (DFT) calculations of dBIP and dBIP-NMe<sub>2</sub> were performed to assist in the understanding of their photophysical properties. As expected, the optimized geometries of both molecules favor the S-trans configuration (Figure S13) and the calculated C-C bond lengths between the two benzothiazole units are 1.45 and 1.44 Å for dBIP and dBIP-NMe<sub>2</sub>, respectively, shorter than a typical C-C single bond (~1.54 Å), implying some extent of conjugation between the two connected benzothiazole units. Because of the electron deficiency of benzothiazole, the lowest unoccupied molecular orbitals (LUMOs) of dBIP and dBIP-NMe<sub>2</sub> are both located on the central bibenzothiazole core with relatively close

energies (-2.78 and -2.65 eV, Figure 2B and Figure S14). However, their highest occupied molecular orbitals (HOMOs) shift from the central benzothiazole region in dBIP to the terminal dimethylaminophenyl groups (PhNMe2) in dBIP-NMe2, in agreement with the electron-donating characteristic of PhNMe<sub>2</sub>. Accordingly, the HOMO of dBIP-NMe<sub>2</sub> (-5.44 eV) lies at 0.65 eV higher than that of dBIP (-6.09 eV). Furthermore, time-dependent DFT (TD-DFT) computations were carried out to shed light on their electronic transitions. For instance, the S<sub>1</sub> state of dBIP was calculated at 372 nm and its electron density difference map (EDDM) suggested its intramolecular charge transfer nature with the central bibenzothiazole core acting as the electron-accepting unit. In addition, other prominent  $S_5$  (f = 0.09) and  $S_7$  (f = 0.81) states of dBIP appearing at 284 and 261 nm, respectively, align very well with the  $n \to \pi^*$  band in its UV-vis absorption spectrum (Figure 2C and Table S1). With the incorporation of those electron-donating -NMe2 substituents, dBIP-NMe2's calculated  $S_1$  state shows a considerable red shift to 429 nm (f =2.64), while other major  $S_3$  and  $S_8$  states are located at 307 nm (f = 0.17) and 283 nm (f = 0.16), respectively (Figure S15 and Table S2).

Encouraged by the photophysical properties of dBIP described above, we first explored its potential application as a one-photon-absorbing photosensitizer in selected organic transformations (Scheme 2) under visible light irradiation ( $\lambda_{ex}$ 

Scheme 2. Photocatalytic Organic Transformations Using dBIP as the Sole Photosensitizer upon Irradiation at 456 nm in the Presence of O<sub>2</sub>

= 456 nm). Our first target reaction was the oxidative upgrading of 5-hydroxymethylfurfural (HMF), a biomass-derived platform chemical. In fact, the electrocatalytic and photocatalytic valorization of HMF has attracted increasing interest of many scientists, <sup>46-51</sup> including our own group, <sup>52-56</sup> and the most common oxidation product of HMF is either 2,5-furandicarboxylic acid or 2,5-diformylfuran. Other value-added fine chemicals like maleic acid anhydride (MA) and 5-hydroxy-

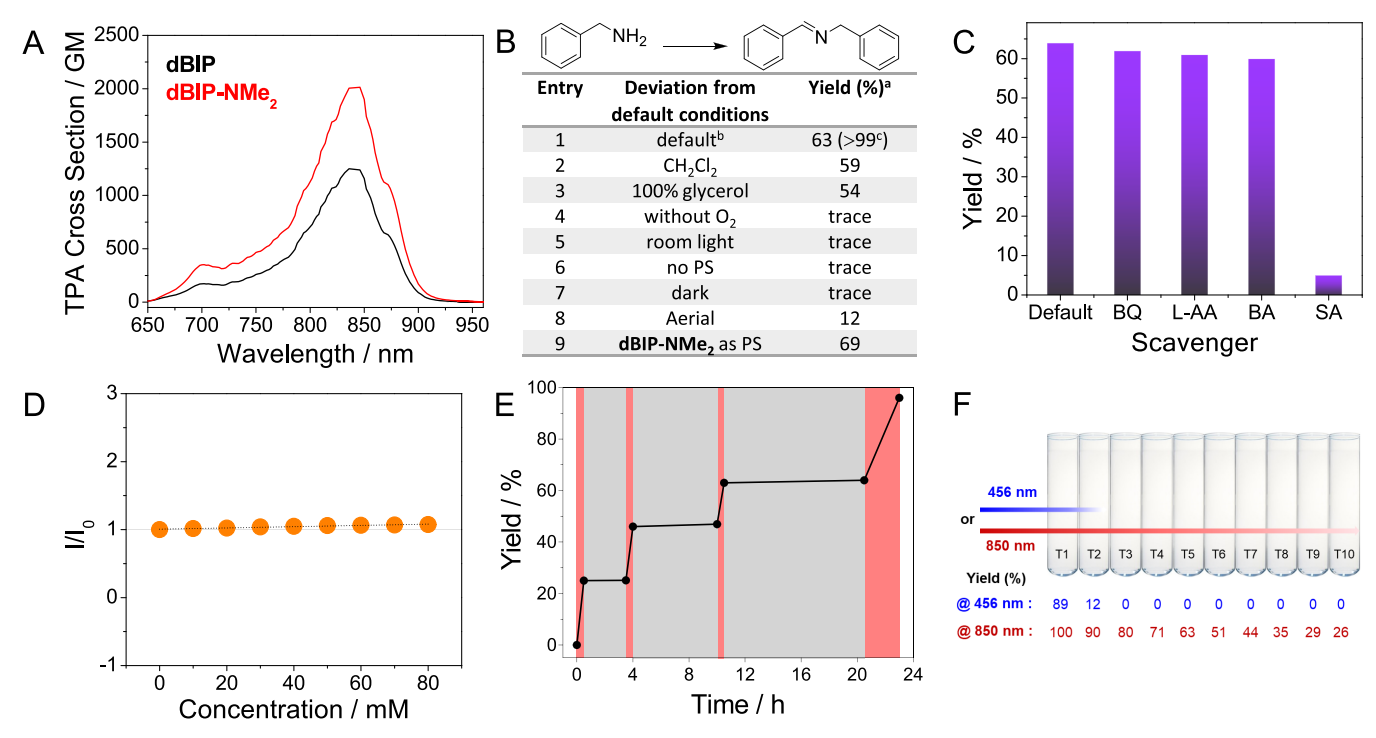


Figure 3. (A) Two-photon absorption cross-section profiles of dBIP and dBIP-NMe<sub>2</sub>. (B) Control experiment results of photocatalytic homocoupling of benzylamine under various conditions. <sup>a</sup>The yields were determined by <sup>1</sup>H NMR analysis. <sup>b</sup>Default reaction conditions: 50 mM benzylamine, 0.5 mol % dBIP as the photosensitizer, O<sub>2</sub>-saturated acetonitrile (2 mL), room temperature, irradiation at 850 nm for 1.5 h. <sup>c</sup>Calculated yield after 5 h irradiation at 850 nm. (C) The yield comparison of benzylamine homocoupling in the presence of various scavengers (100 mM). Default: no scavenger; BQ: benzoquinone; L-AA: L-ascorbic acid; BA: p-chlorobenzoic acid; SA: sodium azide. (D) Stern–Volmer plot of dBIP emission upon the addition of benzylamine. (E) Benzylamine homocoupling yield evolution during the on/off cycles of irradiation at 850 nm. On: red; off: gray. (F) Penetration effect of 456 versus 850 nm irradiation for 10 h on the homocoupling yields of benzylamine with dBIP as the photosensitizer in 10 bundled reaction tubes.

4-keto-2-pentenoic acid (HKPA) have been rarely achieved from the oxidative upgrading of HMF. Herein, we demonstrate that using dBIP as the sole photosensitizer, visible light irradiation was able to drive the transformation of HMF to MA and HKPA with yields of 46% and 50%, respectively, in the presence of O<sub>2</sub> within 6 h (Figure S16). In addition, using O<sub>2</sub> as a green oxidant, dBIP was also able to catalyze the oxidation of thioanisole to methyl phenyl sulfoxide (Figure S17) and cyclohexene to cyclohexene epoxide (Figure S18) with almost quantitative yields after 4 h irradiation at 456 nm. Furthermore, nearly complete photocatalytic C-N crosscoupling between 1-iodo-4-nitrobenzene and piperidine can also be realized using dBIP as the sole photosensitizer within 5 h irradiation at 456 nm (Figure S19). Finally, we found that dBIP was equally effective in driving the homocoupling of benzylamine under O2 upon irradiation at 456 nm, achieving >99% yield within merely 1.2 h (Figure S20). Elongating the photocatalysis duration led to the overoxidation of Nbenzylidenebenzylamine.

Encouraged by the excellent photocatalytic performance of dBIP in driving various  $O_2$ -involved reactions under visible light irradiation, we next sought to explore its potential as a two-photon-absorbing photosensitizer active in the NIR region. Based on its TPA cross section ( $\sigma_2$ ) profile measured from 650 to 950 nm (Figure 3A), dBIP exhibited its maximum  $\sigma_2$  above 1200 GM in the range of 825–855 nm. The more electron-donating  $-NMe_2$  substituents further improved the  $\sigma_2$  of dBIP-NMe<sub>2</sub> to approach 2000 GM in the same region. Hereby, we decided to explore the homocoupling of benzylamine as a model reaction and employ inexpensive

850 nm LED (Thorlabs, 1.4–1.6 W) as the sole light source in all the following photocatalysis experiments. To our delight, as shown in Figure 3B, dBIP was able to convert benzylamine to N-benzylidenebenzylamine with a yield of 63% in O<sub>2</sub>-saturated acetonitrile within 1.5 h irradiation at 850 nm (entry 1). A similar percentage of yield was obtained while using CH<sub>2</sub>Cl<sub>2</sub> as the solvent (entry 2) while it was decreased to 54% in 100% glycerol, which might be due to the slow diffusion of O2 in this highly viscous medium (entry 3). Control experiments conducted in the absence of O2 (entry 4), LED (entry 5), dBIP (entry 6), or dark (entry 7) did not produce any desirable product. A smaller yield was obtained under atmospheric O<sub>2</sub> (~12%, entry 8), implying the crucial need of O<sub>2</sub> in the reaction. An increased yield to 69% (entry 9) was noticed while using dBIP-NMe, as the photosensitizer under the same condition, which is likely due to the better TPA capability of dBIP-NMe2 compared to dBIP (Figure 3A and Figure S21).

Further control experiments performed in the presence of various scavengers, including benzoquinone, L-ascorbic acid, and *p*-chlorobenzoic acid, which are  $O_2^{-\bullet}$ ,  $O_2^-$ , and  $OH^{-\bullet}$  scavengers, respectively, indicated that none of them led to an appreciable yield decrease in benzylamine homocoupling (Figure 3C). However, upon the addition of sodium azide, a  $^1O_2$  scavenger, the yield decreased from 63% to 5% after 1.5 h irradiation at 850 nm (Figure S22), in agreement with the reported results that  $^1O_2$  can drive the oxidative homocoupling of benzylamine to produce *N*-benzylidenebenzylamine. Sa plausible mechanism is included in Scheme S1. This conclusion is also consistent with the fact that no electron

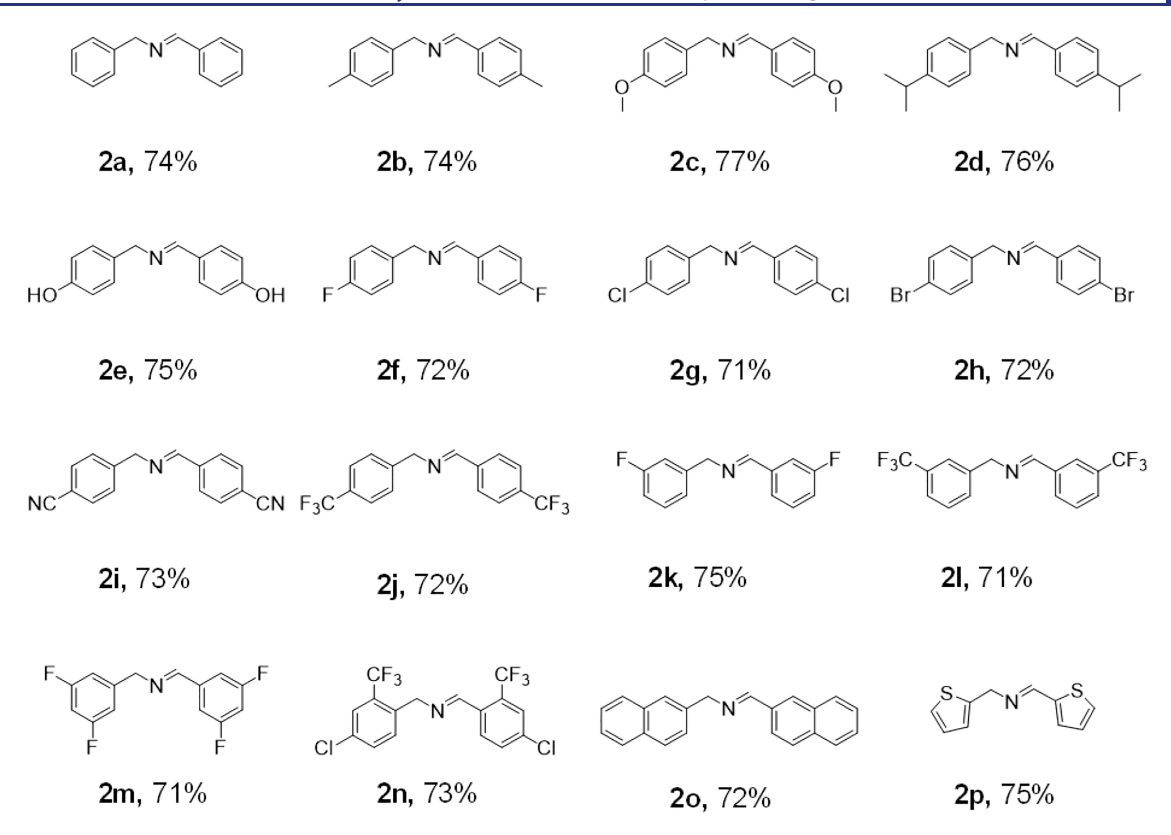


Figure 4. Photocatalytic homocoupling of benzylamine and its derivatives using 0.5 mol % dBIP as the photosensitizer in  $O_2$ -saturated acetonitrile upon 850 nm irradiation for 2 h.

transfer quenching was detected for the emission of dBIP with the addition of benzylamine, as shown in Figure 3D. In fact, appreciable  $^{1}O_{2}$  quantum yields of 0.41 and 0.48 were measured for dBIP and dBIP-NMe<sub>2</sub>, respectively, following the 1,3-diphenylisobenzofuran assay<sup>59</sup> (see details in the Supporting Information, Figures S23 and S24). These above results collectively demonstrate that under 850 nm irradiation, excited dBIP and dBIP-NMe<sub>2</sub> are able to activate  $^{3}O_{2}$  through an energy transfer process to produce  $^{1}O_{2}$ , which drives the homocoupling of benzylamine. The improved performance of dBIP-NMe<sub>2</sub> is likely due to its better TPA, longer lifetime, and hence larger  $^{1}O_{2}$  quantum yield.

The stability and light sensitivity of dBIP for the benzylamine homocoupling reaction were investigated using the "on/off" cycles of 850 nm irradiation. As plotted in Figure 3E, the N-benzylidenebenzylamine yield increased during the light-on periods while it stopped when the light was off. Even after 10 h in the dark, the yield was resumed to increase when the 850 nm LED was turned on again, approaching 100% after accumulative 5 h irradiation overnight (Figure S25). The photostability of dBIP was also assessed by monitoring its <sup>1</sup>H NMR spectral evolution in deaerated CDCl<sub>3</sub> upon 850 nm irradiation over a period of 24 h, and no apparent spectral change was observed (Figure S26).

Next, we sought to compare the photocatalytic performance of dBIP for benzylamine homocoupling upon irradiation with a one-photon (456 nm) versus a two-photon (850 nm) light source. Specifically, 10 reaction tubes were bundled in one row and the irradiation light was only allowed to excite the reaction tubes from the left side while all the other sides were covered by an aluminum foil. The yield of each reaction tube after 10 h irradiation at either 456 or 850 nm is shown in Figure 3F. It is

apparent that the one-photon light source (456 nm) was only able to achieve a decent yield (89%) in the first reaction tube while the second tube already showed a substantially decreased yield of only 12%. All the remaining tubes exhibited no conversion at all, due to the limited penetration of the 456 nm light. In striking contrast, the 850 nm irradiation was able to produce not only 100% yield in the first tube but also decent yields in the second (90%), third (80%), and fourth (71%) tubes. Even the last tube also produced a yield of 26%. These results unambiguously demonstrate the advantages of NIR light irradiation using dBIP as a TPA photosensitizer (Figures S27 and S28).

Besides benzylamine, its close analogues with varying electronic substituents were also subjected to the same photocatalysis condition (850 nm irradiation for 2 h in O<sub>2</sub>saturated acetonitrile) using dBIP as the photosensitizer. As disclosed in Figure 4, with the amendment of different electron-donating groups at the para-position, like -Me (2b), -OMe(2c), and isopropyl (2d), similar yields (74-76%) can be obtained as using the parent benzylamine (2a, 74%). Furthermore, various electron-withdrawing substituents, such as  $-\text{OH}\ (2e),\,-\text{F}\ (2f),\,-\text{Cl}\ (2g),\,-\text{Br}\ (2h),\,-\text{CN}\ (2i),$  and  $-CF_3$  (2j), positioned at either para- or ortho-positions (2k and 21) led to equally decent yields (71–75%) under the same photocatalytic condition. Even in substrates (2m and 2n) with two electron-withdrawing substituents  $(-F, -Cl, and -CF_3)$ at both para- and ortho-positions, excellent yields (71-73%) can still be achieved. In addition to benzylamine derivatives, 2naphthylamine (20) and 2-thiophenemethylamine (2p) can also be homocoupled using dBIP as the photosensitizer upon 2 h irradiation at 850 nm with yields of 72 and 75%, respectively (Figures S29–S44).

#### CONCLUSIONS

In summary, we have reported two novel organic two-photonabsorbing photosensitizers consisting of a bibenzothiazole core as the electron-accepting unit bridged with two phenyl substituents through imine linkages as the electron-donating moieties. Such a  $D-\pi-A-\pi-D$  structure has been demonstrated to result in excellent TPA capability in the NIR region. Hence, a variety of O2-involved energy-transfer organic reactions can be realized using these TPA photosensitizers upon irradiation of 850 nm LED. By changing the terminal substituents, we also demonstrate that a stronger electron donor led to better photocatalytic activity, primarily due to better TPA and longer excited-state lifetime. Because of the deeper penetration and less competing absorption by substrates and media when using NIR photons as the light source, it is anticipated that noble metal-free organic TPA complexes will attract increasing interest in the burgeoning field of organic photocatalysis.

#### ASSOCIATED CONTENT

#### **5** Supporting Information

The Supporting Information is available free of charge at https://pubs.acs.org/doi/10.1021/jacs.2c12244.

Methods for the synthesis, characterization, and photophysical studies of photosensitizers; DFT calculation details; NMR spectra of organic compounds involved in this study (PDF)

#### AUTHOR INFORMATION

#### **Corresponding Author**

Yujie Sun — Department of Chemistry, University of Cincinnati, Cincinnati, Ohio 45221, United States; orcid.org/0000-0002-4122-6255; Email: yujie.sun@uc.edu

#### **Authors**

Bidyut Kumar Kundu — Department of Chemistry, University of Cincinnati, Cincinnati, Ohio 45221, United States; orcid.org/0000-0002-1740-8315

Guanqun Han – Department of Chemistry, University of Cincinnati, Cincinnati, Ohio 45221, United States

Complete contact information is available at: https://pubs.acs.org/10.1021/jacs.2c12244

#### **Author Contributions**

The manuscript was written through contributions of all authors. All authors have given approval to the final version of the manuscript.

#### Notes

The authors declare no competing financial interest.

#### ACKNOWLEDGMENTS

Y.S. acknowledges the support of the National Science Foundation (CHE-1955358), University of Cincinnati, and the Ohio Supercomputer Center.

#### REFERENCES

(1) Kärkäs, M. D.; Porco, J. A.; Stephenson, C. R. J. Photochemical approaches to complex chemotypes: applications in natural product synthesis. *Chem. Rev.* **2016**, *116*, 9683–9747.

- (2) Capaldo, L.; Ravelli, D.; Fagnoni, M. Direct photocatalyzed hydrogen atom transfer (HAT) for aliphatic C–H bonds elaboration. *Chem. Rev.* **2022**, *122*, 1875–1924.
- (3) Candish, L.; Collins, K. D.; Cook, G. C.; Douglas, J. J.; Gómez-Suárez, A.; Jolit, A.; Keess, S. Photocatalysis in the life science industry. *Chem. Rev.* **2022**, *122*, 2907–2980.
- (4) Lechner, V. M.; Nappi, M.; Deneny, P. J.; Folliet, S.; Chu, J. C. K.; Gaunt, M. J. Visible-light-mediated modification and manipulation of biomacromolecules. *Chem. Rev.* **2022**, *122*, 1752–1829.
- (5) Samokhvalov, A. Desulfurization of real and model liquid fuels using light: photocatalysis and photochemistry. *Catal. Rev.* **2012**, *54*, 281–343.
- (6) Buglioni, L.; Raymenants, F.; Slattery, A.; Zondag, S. D. A.; Noël, T. Technological innovations in photochemistry for organic synthesis: flow chemistry, high-throughput experimentation, scale-up, and photoelectrochemistry. *Chem. Rev.* **2022**, *122*, 2752–2906.
- (7) Narayanam, J. M. R.; Stephenson, C. R. J. Visible light photoredox catalysis: applications in organic synthesis. *Chem. Soc. Rev.* **2011**, *40*, 102–113.
- (8) Prier, C. K.; Rankic, D. A.; MacMillan, D. W. C. Visible light photoredox catalysis with transition metal complexes: applications in organic synthesis. *Chem. Rev.* **2013**, *113*, 5322–5363.
- (9) Twilton, J.; Le, C.; Zhang, P.; Shaw, M. H.; Evans, R. W.; MacMillan, D. W. C. The merger of transition metal and photocatalysis. *Nat. Rev. Chem.* 2017, 1, 0052.
- (10) Arias-Rotondo, D. M.; McCusker, J. K. The photophysics of photoredox catalysis: a roadmap for catalyst design. *Chem. Soc. Rev.* **2016**, 45, 5803–5820.
- (11) Albini, A.; Fagnoni, M. Photochemically-generated intermediate in synthesis, Willey. VCH, Weinheim: 2013.
- (12) Chan, A. Y.; Perry, I. B.; Bissonnette, N. B.; Buksh, B. F.; Edwards, G. A.; Frye, L. I.; Garry, O. L.; Lavagnino, M. N.; Li, B. X.; Liang, Y.; Mao, E.; Millet, A.; Oakley, J. V.; Reed, N. L.; Sakai, H. A.; Seath, C. P.; MacMillan, D. W. C. Metallaphotoredox: the merger of photoredox and transition metal catalysis. *Chem. Rev.* **2022**, *122*, 1485–1542.
- (13) Le, C. C.; Wismer, M. K.; Shi, Z.-C.; Zhang, R.; Conway, D. V.; Li, G.; Vachal, P.; Davies, I. W.; MacMillan, D. W. C. A general small-scale reactor to enable standardization and acceleration of photocatalytic reactions. *ACS Cent. Sci.* **2017**, *3*, 647–653.
- (14) Ravetz, B. D.; Tay, N. E. S.; Joe, C. L.; Sezen-Edmonds, M.; Schmidt, M. A.; Tan, Y.; Janey, J. M.; Eastgate, M. D.; Rovis, T. Development of a platform for near-infrared photoredox catalysis. *ACS Cent. Sci.* **2020**, *6*, 2053–2059.
- (15) González-Esguevillas, M.; Fernández, D. F.; Rincón, J. A.; Barberis, M.; de Frutos, O.; Mateos, C.; García-Cerrada, S.; Agejas, J.; MacMillan, D. W. C. Rapid optimization of photoredox reactions for continuous-flow systems using microscale batch technology. *ACS Cent. Sci.* **2021**, *7*, 1126–1134.
- (16) Gisbertz, S.; Reischauer, S.; Pieber, B. Overcoming limitations in dual photoredox/nickel-catalysed C–N cross-couplings due to catalyst deactivation. *Nat. Catal.* **2020**, *3*, 611–620.
- (17) McNamara, W. R.; Han, Z.; Alperin, P. J.; Brennessel, W. W.; Holland, P. L.; Eisenberg, R. A Cobalt—dithiolene complex for the photocatalytic and electrocatalytic reduction of protons. *J. Am. Chem. Soc.* **2011**, *133*, 15368–15371.
- (18) McNamara, W. R.; Han, Z.; Yin, C.-J.; Brennessel, W. W.; Holland, P. L.; Eisenberg, R. Cobalt-dithiolene complexes for the photocatalytic and electrocatalytic reduction of protons in aqueous solutions. *Proc. Natl. Acad. Sci. U. S. A.* **2012**, *109*, 15594–15599.
- (19) Ahmad, I.; Ahmed, S.; Anwar, Z.; Sheraz, M. A.; Sikorski, M. Photostability and photostabilization of drugs and drug products. *Int. J. Photoenergy* **2016**, *2016*, 8135608.
- (20) Romero, N. A.; Nicewicz, D. A. Organic photoredox catalysis. *Chem. Rev.* **2016**, *116*, 10075–10166.
- (21) Leung, C.-F.; Lau, T.-C. Organic photosensitizers for catalytic solar fuel generation. *Energy Fuels* **2021**, *35*, 18888–18899.

- (22) Ghosh, A.; Pyne, P.; Ghosh, S.; Ghosh, D.; Majumder, S.; Hajra, A. Visible-light-induced metal-free coupling of C(sp<sup>3</sup>)–H sources with heteroarenes. *Green Chem.* **2022**, *24*, 3056–3080.
- (23) Strehmel, B.; Schmitz, C.; Cremanns, K.; Göttert, J. Photochemistry with cyanines in the near infrared: a step to Chemistry 4. 0 technologies. *Chem. Eur. J.* **2019**, 25, 12855–12864.
- (24) Kosso, A. R. O.; Sellet, N.; Baralle, A.; Cormier, M.; Goddard, J.-P. Cyanine-based near infrared organic photoredox catalysis. *Chem. Sci.* **2021**, *12*, 6964–6968.
- (25) Zhou, J.; Liu, Q.; Feng, W.; Sun, Y.; Li, F. Upconversion luminescent materials: advances and applications. *Chem. Rev.* **2015**, 115, 395–465.
- (26) Ravetz, B. D.; Pun, A. B.; Churchill, E. M.; Congreve, D. N.; Rovis, T.; Campos, L. M. Photoredox catalysis using infrared light via triplet fusion upconversion. *Nature* **2019**, *565*, 343–346.
- (27) Huang, L.; Wu, W.; Li, Y.; Huang, K.; Zeng, L.; Lin, W.; Han, G. Highly effective near-infrared activating triplet—triplet annihilation upconversion for photoredox catalysis. *J. Am. Chem. Soc.* **2020**, *142*, 18460—18470.
- (28) Huang, L.; Zeng, L.; Chen, Y.; Yu, N.; Wang, L.; Huang, K.; Zhao, Y.; Han, G. Long wavelength single photon like driven photolysis via triplet triplet annihilation. *Nat. Commun.* **2021**, *12*, 122.
- (29) Glaser, F.; Kerzig, C.; Wenger, O. S. Multi-photon excitation in photoredox catalysis: concepts, applications, methods. *Angew. Chem., Int. Ed.* **2020**, *59*, 10266–10284.
- (30) Han, G.; Li, G.; Huang, J.; Han, C.; Turro, C.; Sun, Y. Two-photon-absorbing ruthenium complexes enable near infrared light-driven photocatalysis. *Nat. Commun.* **2022**, *13*, 2288.
- (31) Park, Y. I.; Lee, K. T.; Suh, Y. D.; Hyeon, T. Upconverting nanoparticles: a versatile platform for wide-field two-photon microscopy and multi-modal in vivo imaging. *Chem. Soc. Rev.* **2015**, 44, 1302–1317.
- (32) Xu, L.; Zhang, J.; Yin, L.; Long, X.; Zhang, W.; Zhang, Q. Recent progress in efficient organic two-photon dyes for fluorescence imaging and photodynamic therapy. *J. Mater. Chem. C* **2020**, *8*, 6342–6349.
- (33) Zhang, Q.; Lu, X.; Cao, H.; Wang, H.; Zhu, T.; Tian, X.; Li, D.; Zhou, H.; Wu, J.; Tian, Y. Multiphoton absorption iridium(III)—organotin(IV) dimetal complex with AIE behavior for both sensitive detection of tyrosine and antibacterial activity. ACS Appl. Bio Mater. 2020, 3, 8105–8112.
- (34) Pawlicki, M.; Collins, H. A.; Denning, R. G.; Anderson, H. L. Two-photon absorption and the design of two-photon dyes. *Angew. Chem. Int. Ed.* **2009**, *48*, 3244–3266.
- (35) Zhou, R.; Malval, J.-P.; Jin, M.; Spangenberg, A.; Pan, H.; Wan, D.; Morlet-Savary, F.; Knopf, S. A two-photon active chevron-shaped type I photoinitiator designed for 3D stereolithography. *Chem. Commun.* **2019**, *55*, 6233–6236.
- (36) Albota, M.; Beljonne, D.; Brédas, J.-L.; Ehrlich, J. E.; Fu, J.-Y.; Heikal, A. A.; Hess, S. E.; Kogej, T.; Levin, M. D.; Marder, S. R.; McCord-Maughon, D.; Perry, J. W.; Röckel, H.; Rumi, M.; Subramaniam, G.; Webb, W. W.; Wu, X.-L.; Xu, C. Design of organic molecules with large two-photon absorption cross sections. *Science* 1998, 281, 1653.
- (37) Xu, L.; Lin, W.; Huang, B.; Zhang, J.; Long, X.; Zhang, W.; Zhang, Q. The design strategies and applications for organic multibranched two-photon absorption chromophores with novel cores and branches: a recent review. *J. Mater. Chem. C* **2021**, *9*, 1520–1536.
- (38) Gautam, P.; Wang, Y.; Zhang, G.; Sun, H.; Chan, J. M. W. Using the negative hyperconjugation effect of pentafluorosulfanyl acceptors to enhance two-photon absorption in push—pull chromophores. *Chem. Mater.* **2018**, *30*, 7055—7066.
- (39) Pérez-Caaveiro, C.; Oliva, M. M.; López Navarrete, J. T.; Pérez Sestelo, J.; Martínez, M. M.; Sarandeses, L. A. Synthesis of D–A–A and D–A–D pyrimidine  $\pi$ -systems using triorganoindium reagents: optical, vibrational, and electrochemical studies. *J. Org. Chem.* **2019**, 84, 8870–8885.
- (40) Nociarová, J.; Osuský, P.; Rakovský, E.; Georgiou, D.; Polyzos, I.; Fakis, M.; Hrobárik, P. Direct iodination of electron-deficient

- benzothiazoles: rapid access to two-photon absorbing fluorophores with quadrupolar D-π-A-π-D architecture and tunable heteroaromatic Core. *Org. Lett.* **2021**, *23*, 3460–3465.
- (41) Hrobárik, P.; Hrobáriková, V.; Sigmundová, I.; Zahradník, P.; Fakis, M.; Polyzos, I.; Persephonis, P. Benzothiazoles with tunable electron-withdrawing strength and reverse polarity: a route to triphenylamine-based chromophores with enhanced two-photon absorption. *J. Org. Chem.* **2011**, *76*, 8726–8736.
- (42) Hrobárik, P.; Hrobáriková, V.; Semak, V.; Kasák, P.; Rakovský, E.; Polyzos, I.; Fakis, M.; Persephonis, P. Quadrupolar benzobisthiazole-cored arylamines as highly efficient two-photon absorbing fluorophores. *Org. Lett.* **2014**, *16*, 6358–6361.
- (43) Osuský, P.; Nociarová, J.; Smolíček, M.; Gyepes, R.; Georgiou, D.; Polyzos, I.; Fakis, M.; Hrobárik, P. Oxidative C—H homocoupling of push—pull benzothiazoles: an atom-economical route to highly emissive quadrupolar arylamine-functionalized 2,2′-bibenzothiazoles with enhanced two-photon absorption. *Org. Lett.* **2021**, 23, 5512—5517.
- (44) Yang, Y.; Lan, J.; You, J. Oxidative C-H/C-H coupling reactions between two (hetero)arenes. *Chem. Rev.* **2017**, *117*, 8787–8863
- (45) Rurack, K.; Spieles, M. Fluorescence quantum yields of a series of red and near-infrared dyes emitting at 600–1000 nm. *Anal. Chem.* **2011**, 83, 1232–1242.
- (46) Rosatella, A. A.; Simeonov, S. P.; Frade, R. F. M.; Afonso, C. A. M. 5-Hydroxymethylfurfural (HMF) as a building block platform: Biological properties, synthesis and synthetic applications. *Green Chem.* **2011**, *13*, 754–793.
- (47) van Putten, R.-J.; van der Waal, J. C.; de Jong, E.; Rasrendra, C. B.; Heeres, H. J.; de Vries, J. G. Hydroxymethylfurfural, a versatile platform chemical made from renewable resources. *Chem. Rev.* **2013**, 113, 1499–1597.
- (48) Cha, H. G.; Choi, K.-S. Combined biomass valorization and hydrogen production in a photoelectrochemical cell. *Nat. Chem.* **2015**, 7, 328–333.
- (49) Krivtsov, I.; García-López, E. I.; Marcì, G.; Palmisano, L.; Amghouz, Z.; García, J. R.; Ordóñez, S.; Díaz, E. Selective photocatalytic oxidation of 5-hydroxymethyl-2-furfural to 2,5-furandicarboxyaldehyde in aqueous suspension of g-C<sub>3</sub>N<sub>4</sub>. *Appl. Catal. B: Environ.* **2017**, 204, 430–439.
- (50) Zhang, H.; Wu, Q.; Guo, C.; Wu, Y.; Wu, T. Photocatalytic selective oxidation of 5-hydroxymethylfurfural to 2,5-diformylfuran over Nb<sub>2</sub>O<sub>5</sub> under visible light. ACS Sustainable Chem. Eng. **2017**, 5, 3517–3523.
- (51) Kisszekelyi, P.; Hardian, R.; Vovusha, H.; Chen, B.; Zeng, X.; Schwingenschlögl, U.; Kupai, J.; Szekely, G. Selective electrocatalytic oxidation of biomass-derived 5-hydroxymethylfurfural to 2,5-diformylfuran: from mechanistic investigations to catalyst recovery. *ChemSusChem* **2020**, *13*, 3127–3136.
- (52) Jiang, N.; You, B.; Boonstra, R.; Terrero Rodriguez, I. M.; Sun, Y. Integrating electrocatalytic 5-hydroxymethylfurfural oxidation and hydrogen production via Co–P-derived electrocatalysts. *ACS Energy Lett.* **2016**, *1*, 386–390.
- (53) You, B.; Liu, X.; Jiang, N.; Sun, Y. A general strategy for decoupled hydrogen production from water splitting by integrating oxidative biomass valorization. *J. Am. Chem. Soc.* **2016**, *138*, 13639–13646.
- (54) You, B.; Jiang, N.; Liu, X.; Sun, Y. Simultaneous  $H_2$  generation and biomass upgrading in water by an efficient noble-metal-free bifunctional electrocatalyst. *Angew. Chem., Int. Ed.* **2016**, *55*, 9913–9917.
- (55) Han, G.; Jin, Y.-H.; Burgess, R. A.; Dickenson, N. E.; Cao, X.-M.; Sun, Y. Visible-light-driven valorization of biomass intermediates integrated with H<sub>2</sub> production catalyzed by ultrathin Ni/CdS nanosheets. *J. Am. Chem. Soc.* **2017**, *139*, 15584–15587.
- (56) Li, W.; Jiang, N.; Hu, B.; Liu, X.; Song, F.; Han, G.; Jordan, T. J.; Hanson, T. B.; Liu, T. L.; Sun, Y. Electrolyzer design for flexible decoupled water splitting and organic upgrading with electron reservoirs. *Chem* **2018**, *4*, 637–649.

- (57) Deol, H.; Singh, G.; Kumar, M.; Bhalla, V. Phenazine-based donor acceptor systems as organic photocatalysts for "metal-free" C-N/C-C cross-coupling. J. Org. Chem. 2020, 85, 11080-11093.
- (58) Xu, C.; Liu, H.; Li, D.; Su, J.-H.; Jiang, H.-L. Direct evidence of charge separation in a metal-organic framework: efficient and selective photocatalytic oxidative coupling of amines via charge and energy transfer. Chem. Sci. 2018, 9, 3152-3158.
- (59) Nguyen, V.-N.; Qi, S.; Kim, S.; Kwon, N.; Kim, G.; Yim, Y.; Park, S.; Yoon, J. An emerging molecular design approach to heavyatom-free photosensitizers for enhanced photodynamic therapy under hypoxia. J. Am. Chem. Soc. 2019, 141, 16243-16248.

### Recommended by ACS

Long-Wavelength Photoconvertible Dimeric BODIPYs for **Super-Resolution Single-Molecule Localization Imaging in Near-Infrared Emission** 

Qingbao Gong, Erhong Hao, et al.

NOVEMBER 22, 2022

JOURNAL OF THE AMERICAN CHEMICAL SOCIETY

READ **Z** 

**Bodipy-Based Metal-Organic Frameworks Transformed in** Solid States from 1D Chains to 2D Layer Structures as Efficient Visible Light Heterogeneous Photocatalysts for...

Qingchun Xia, Xuenian Chen, et al.

MARCH 13, 2023

JOURNAL OF THE AMERICAN CHEMICAL SOCIETY

READ **C** 

#### Recent Progress and Trends in X-ray-Induced Photodynamic Therapy with Low Radiation Doses

Liangrui He, Wanwan Li, et al.

NOVEMBER 15, 2022

ACS NANO

READ 🗹

#### The Overlooked Photochemistry of Iodine in Aqueous **Suspensions of Fullerene Derivatives**

Madhusudan Kamat, Samuel D. Snow, et al.

MAY 09, 2022

ACS NANO

READ

Get More Suggestions >